

# Thrust Modulation in a Nitrous-Oxide/Hydroxyl-Terminated Polybutadiene Hybrid Rocket Motor

Rajesh K. K.\*

*Defense Research and Development Laboratory  
Hyderdabad – 500 058, India*

The design details of a hybrid rocket motor for a specified thrust time profile are described. The oxidizer chosen is Nitrous Oxide ( $N_2O$ ) and the fuel is Hydroxyl-Terminated Polybutadiene (HTPB). The design of the motor is based on a code realized for predicting the performance of the hybrid rocket motor. A regression rate correlation derived for Gaseous Oxygen/HTPB system has been used in the absence of any useful experimental regression rate data on  $N_2O$ /HTPB system. The characteristics of the combustion products are calculated using the code NASA CEA and curve fitted as a function of oxidizer/fuel ratio. The geometry and the oxidizer mass flow requirements of the hybrid motor for a given mission are brought out. The capability of the hybrid rocket motor for thrust modulation is well demonstrated.

## Nomenclature

$a$	= exponent in regression rate correlation
$A_b$	= regressing surface area, $m^2$
$A_e$	= nozzle exit area, $m^2$
$A_p$	= port area, $m^2$
$A_t$	= nozzle throat area, $m^2$
$c^*$	= characteristic velocity, m/s
$c_{exp}^*$	= experimental characteristic velocity, m/s
$C_F$	= thrust coefficient
$D_p$	= port diameter, m
$G_o$	= oxidizer mass flux, $kg/m^2s$
$L$	= length of grain, m
$m_a$	= mass accumulation rate, kg/s
$m_f$	= mass flow rate of fuel, kg/s
$m_o$	= mass flow rate of oxidizer, kg/s
$m_n$	= mass flow rate through nozzle throat, kg/s
$M$	= molecular weight of combustion products
$n$	= index in regression rate correlation
$P_a$	= ambient pressure, Pa
$P_c$	= chamber pressure, Pa
$P_e$	= nozzle exit pressure, Pa
$r$	= regression rate, m/s
$R$	= port radius, m
$R$	= universal gas constant
$R$	= gas constant of combustion products
$T_c$	= adiabatic flame temperature of combustion products, K
$V_c$	= motor free volume, $m^3$
$\Delta t$	= time increment, s
$\phi$	= oxidizer-fuel ratio
$\rho_c$	= density of combustion products, $kg/m^3$
$\rho_f$	= density of fuel, $kg/m^3$
$\gamma$	= ratio of specific heats of combustion products
$\xi$	= combustion efficiency

## I. Introduction

With their unique operational characteristics, hybrid rockets can potentially provide safer, lower-cost avenues to space than the current solid propellant and liquid propellant systems. In classical hybrid

---

\* Scientist, Solid Rocket & Solid Ramjet Propulsion Division

rocket motors, fuel is in the solid phase and the oxidizer is in the liquid phase. They offer several advantages over their solid and liquid counterparts. Solid fuels are safer than solid propellants on the points of view of manufacture, transportation and storage. Unlike solid rockets, hybrid rockets have the ability to change thrust over a wider range, and to shutdown and restart. Also the performance of hybrid rockets is much less sensitive to cracks and debonds in fuel grains. Relative to liquid engines, hybrid rockets require only half as much feed system hardware and therefore display higher reliability. The commonly used fuels are environment friendly, nontoxic, and not hazardous to store and transport unlike many volatile liquid fuels. Hybrid rockets generally have the values of specific impulse higher than solid rockets and of density specific impulse greater than liquid bi-propellant rockets. Due to these safety and operational advantages, classical hybrid engines could display lower manufacture and launch costs than current propulsion systems.

This paper details the design of a hybrid rocket motor for a specified thrust. The oxidizer and fuel chosen are nitrous oxide ( $N_2O$ ) and hydroxyl-terminated polybutadiene (HTPB) respectively.  $N_2O$  known as Di-Nitrogen Monoxide, as well as laughing gas, has a boiling point of  $-89.5^\circ C$  at 1 atm, and is normally maintained as a liquid at a pressure of about 58 bar. It has a molecular weight of 44.0 and a density of  $1226 \text{ kg/m}^3$  at  $20^\circ C$ . The critical pressure and temperature of  $N_2O$  is 7.27 MPa and  $36.6^\circ C$ . Hybrid motor with  $N_2O$  as oxidizer has an additional advantage that the oxidizer tank does not require a pressurization system because of its self-pressurization characteristics (if the operating pressure is well below 45bar).  $N_2O$  is safer, and inexpensive compared to other oxidizers like liquid oxygen. It has a vapor pressure at ambient temperature that allows two-phase storage and efficient oxidizer delivery through a self-pressuring process. During the discharge of liquid  $N_2O$  the ullage volume increases significantly. As the  $N_2O$  is having relatively high vapour pressure at ambient temperature the hybrid motor can operate at a chamber pressure, which is enough to achieve the required thrust level. Another interesting advantage of  $N_2O$  self-pressuring system is that, it allows the residual ullage gas to combust with fuel even after all of the liquid has been discharged from the tank. Inert gases like Helium can be used to pressurize the  $N_2O$  tank to its saturation pressure to ensure the necessary flow rate, if the operating pressure is more than 45 bar.

In order to design a  $N_2O$ /HTPB hybrid rocket motor, one should know the regression rate characteristics of HTPB under  $N_2O$  environment. Very little information is available in Literature regarding the  $N_2O$ /HTPB hybrid rockets especially experimental correlations. Attempt to derive a regression rate correlation from an experimental work reported very recently has led to some inconsistencies due to the extrapolation from a narrow range of mass flux. In the absence of any other data, an experimental correlation derived for HTPB and Gaseous Oxygen (GOX) from Literature has been used. A code is realized for predicting the performance of the  $N_2O$ /HTPB hybrid rocket motor. The characteristics of the combustion products are calculated using the code NASA CEA and curve fitted as a function of oxidizer/fuel (O/F) ratio. Using the code, performance predictions are obtained for a range of mass flow rates of the oxidizer. Based on these results, the geometry of the hybrid rocket motor and the oxidizer mass flow requirements for a specified dual thrust mode of operation are derived.

## II. Ballistics Code Development

A single port cylindrical grain as shown in Fig. 1 is used for the analysis. The grain is allowed to burn only on the cylindrical surface. Mass flow rate of the  $N_2O$  is assumed constant and can be specified. It is also assumed that the regression rate is constant along the port. The enlargement of the nozzle throat due to erosion is considered zero. As the hybrid motors are characterised by pre and post combustion chambers to ensure better combustion of fuel and oxidizer, the mass accumulation terms are not negelected in the analysis.

At any instant of time t, conservation of mass gives

$$\dot{m}_o + \dot{m}_f = \dot{m}_n + \dot{m}_a \quad (1)$$

in which the fuel flow rate is

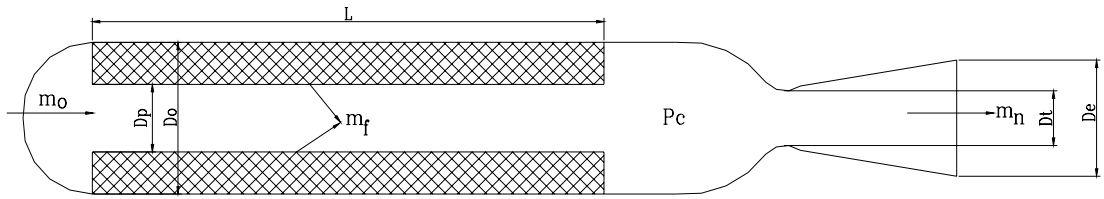


Figure 1. Geometry of the motor considered for the analysis

$$\dot{m}_f = \rho_f A_b \dot{r} \quad (2)$$

where

$$A_b = 2\pi RL \quad (3)$$

Regression rate of a hybrid fuel is generally a function several variables such as oxidizer mass flux ( $G_o$ ), port diameter ( $D_p$ ), axial distance (from leading edge), and pressure etc. Out of these, oxidizer mass flux is the most dominant one and for simplicity expressing regression rate as a function of  $G_o$

$$\dot{r} = aG_o^n \quad (4)$$

where 'a' & 'n' are to be obtained experimentally and .

$$G_o = \frac{\dot{m}_o}{A_p} \quad (5)$$

From the fuel mass flow rate and the known oxidizer mass flow rate obtains the O/F ratio

$$\phi = \frac{\dot{m}_o}{\dot{m}_f} \quad (6)$$

Now  $T_c$ ,  $M$ , and  $\gamma$  can be obtained as a function of  $\phi$  from which the characteristic velocity is obtained as

$$C^* = \frac{\sqrt{RT_c}}{\Gamma} \quad (7)$$

where

$$\Gamma = \sqrt{\gamma \left( \frac{2}{\gamma+1} \right)^{\frac{(\gamma+1)}{2(\gamma-1)}}} \quad (8)$$

and

$$R = \frac{\bar{R}}{M} \quad (9)$$

Experimental characteristic velocity is obtained by assuming a combustion efficiency factor

$$C_{\text{exp}}^* = \xi C^* \quad (10)$$

A combustion efficiency of 0.93 to 0.97 is achieved in various hybrid experiments reported<sup>1</sup>. So  $\xi$  is taken here as 0.93.

Now mass flow through the nozzle is

$$\dot{m}_n = \frac{P_c A_t}{C_{\text{exp}}^*} \quad (11)$$

The mass accumulation term is given by

$$\dot{m}_a = \frac{d(\rho_c V_c)}{dt} \quad (12)$$

Combining the Eqs. (3-5), Eq. 2 can be written as

$$\dot{m}_f = \rho_f A_b a G_o^n \quad (13)$$

Substituting Eqs. (11-13) into Eq. 1 and re-arranging

$$\frac{dP_c}{dt} = \left[ \dot{m}_o + (\rho_f - \rho_c) A_b a G_o^n - \frac{P_c A_t}{C_{\text{exp}}^*} \right] \frac{RT_c}{V_c} \quad (14)$$

and the chamber pressure  $P_c$  can be obtained for any time instant by solving this equation.

Once  $P_c$  is obtained, thrust and specific impulse at that instant are calculated using the standard equations

$$C_F = \sqrt{\frac{2\gamma^2}{(\gamma-1)(\gamma+1)} \left(\frac{2}{\gamma+1}\right)^{\frac{(\gamma+1)}{(\gamma-1)}} \left[1 - \left(\frac{P_e}{P_c}\right)^{\frac{(\gamma-1)}{\gamma}}\right] + \frac{(P_e - P_a) A_e}{P_c A_t}} \quad (15)$$

$$F = C_F P_c A_t \quad (16)$$

and

$$I_{sp} = \frac{F}{\dot{m}} \quad (17)$$

Now, the instantaneous port radius R is obtained as

$$R = R + \dot{r} \Delta t \quad (18)$$

The  $P_c$  at the next time increment can be calculated from Eq.(14) by considering the increase in free volume due to the reduction in the web thickness of the fuel grain. The change in combustion gas density is also considered through the equation

$$\rho_c = \frac{P_c}{RT_c} \quad (19)$$

The iterations will proceed till the instantaneous port radius becomes equal to the outer radius of the grain.

#### A. Regression rate model

No valid correlation for regression rate is available for  $N_2O$ /HTPB system. A recent study<sup>2</sup> conducted at University of Colorado at Boulder by Otto Krauss et al. on  $N_2O$  /HTPB system gives a few experimental data in the form of regression rate vs. oxidizer mass flux, Fig. 2. However, the regression rate correlation derived in the usual form (exponential) based on this limited data appears to be unrealistic because of the resulting regression rate index which is more than unity, Eq. 20 and Fig. 2.

$$\dot{r} = 9.3368 \times 10^{-8} G_o^{1.6386} \quad (20)$$

It is found that the use of this correlation led to some inconsistencies due to the extrapolation from a narrow range of mass flux. In the absence of any other data, it is decided to use an experimental correlation derived by George et al. for HTPB and GOX<sup>3</sup>. The correlation is expressed as follows,

$$\dot{r} = 6.37 \times 10^{-5} G_o^{0.41} D_p^{-0.24} \quad (21)$$

## B. Solution procedure

The specified thrust time profile and the design requirements are given in Table 1. By assuming the motor geometry, thrust time traces are computed till the end of 9.5 s assuming two different levels of oxidizer mass flow rates corresponding to each thrust level. The motor free-volume is assumed on the following basis. It is reported<sup>4</sup> that  $L^*$  values as low as 1.0 m may provide sufficient aft combustion volume for efficiencies more than 90 percent. So the aft-combustion chamber volume is calculated based on an  $L^*$  value of 1.5 m. The pre combustion chamber volume is taken as one third of the aft-combustion chamber volume.

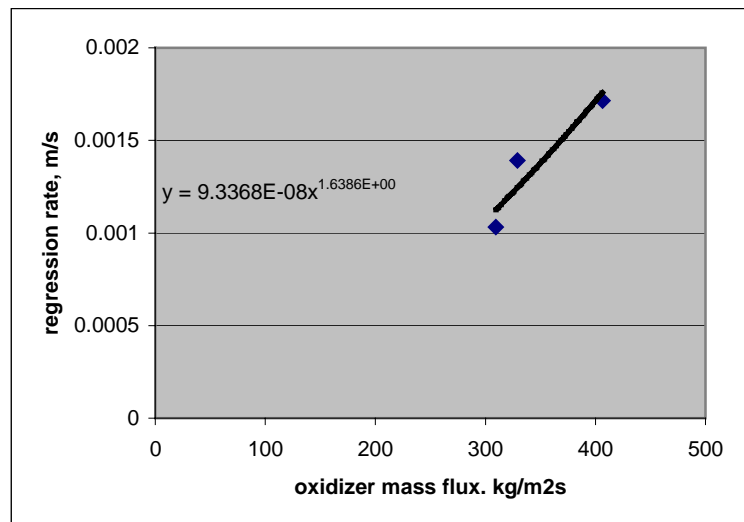


**Figure 2. Regression rate vs. oxidizer mass flux**

These trial and error runs repeated till a good match is obtained between the predicted thrust time trace and the specified one. A method to obtain the approximate oxidizer mass flow rates that are required to begin the trial and error computations is given in Appendix. In the process the exit pressure is kept under check i.e. above the standard sea level value of  $1.01325 \times 10^5$  Pa in order to avoid any possible over-expansion.

**Table 1 Design requirements**

Specification	Numerical values
Thrust during the first phase (5.5 s)	18,000 N
Thrust during the second phase (4s)	8000 N
Fuel grain outer diameter	164 mm

## III. Results

NASA CEA code<sup>5</sup> is run to calculate the characteristics of the combustion products resulting from the combustion of  $N_2O$  and HTPB. The molecular formula and enthalpy of formation of the reactants are obtained from ICT Database of Thermochemical Value<sup>6</sup>. The density of HTPB is taken as  $960 \text{ kg/m}^3$ . The propellant composition is given in Table 2. In hybrid rocket motors, unlike in solid/liquid propellant rocket motors, the O/F ratio changes every instant. So the characteristics of the  $N_2O$ /HTPB combustion products are to be obtained as a function of O/F ratio from the CEA code. The characteristics of the combustion products are obtained for a number of O/F values ranging from 0.5 to 10 at an interval of 0.5 and curve fitted, assuming a chamber pressure of 70 bar and equilibrium flow, Figs. 3, 4, & 5.

**Table 2 Propellant composition and specification**

Reactants	% wt	Heat of formation, cal/mole	Phase	Initial temperature, K
$N_2O$	100	15500	Liquid	298.15
$C_{7.1102}H_{10.813}N_{0.1071}O_{0.1375}$	100	-7541	Solid	298.15

**Table 3 Characteristics of combustion products (O/F ratio = 7.0)**

Characteristics	Numerical values
Adiabatic flame temperature, K	3467.62
Molecular weight, g/mol	26.88
Ratio of specific heats	1.1546

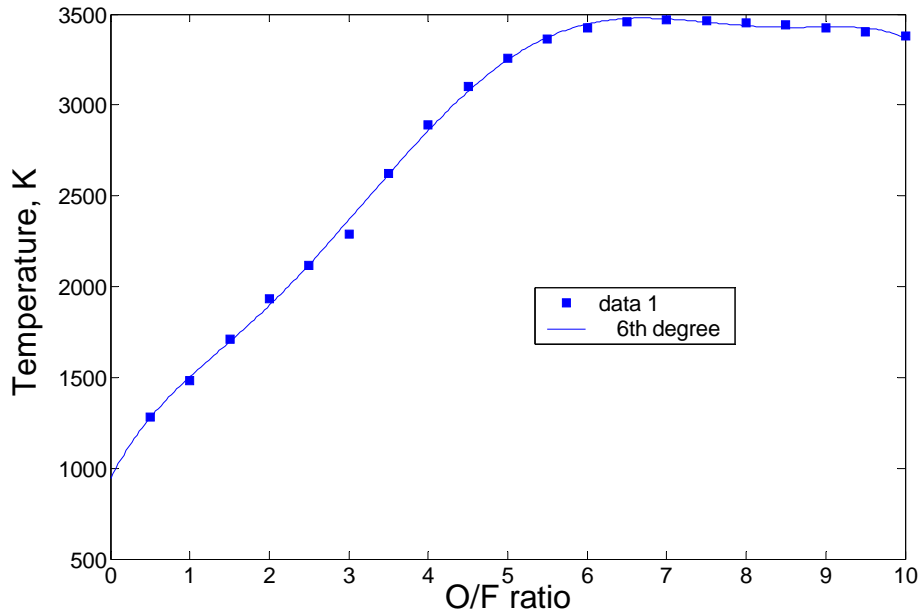


**Figure 3. Adiabatic flame temperature vs. O/F ratio**

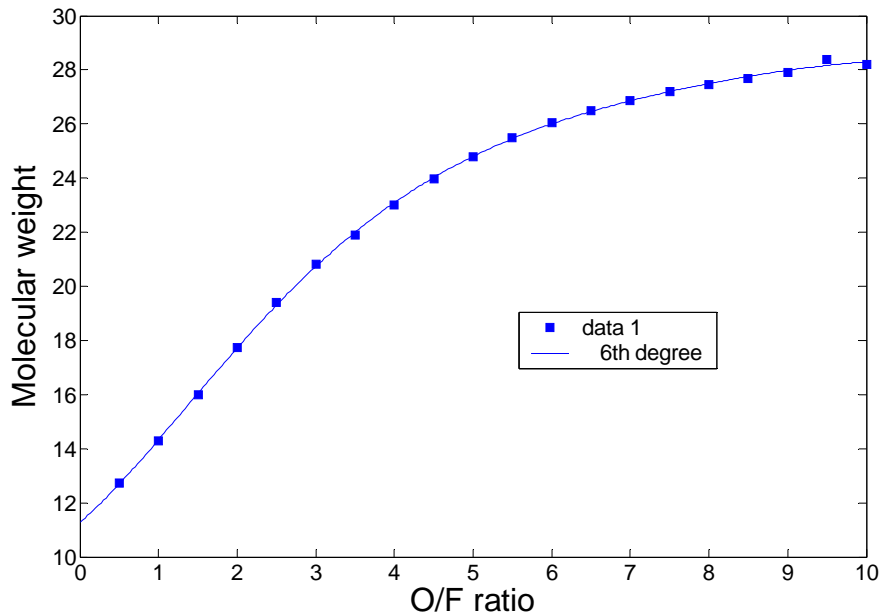


**Figure 4. Molecular weight vs. O/F ratio**

These curve fits are demonstrated to be valid over a range of pressures from 25 to 100 bars on account of the insensitivity of these characteristics to chamber pressure. Characteristics of the N<sub>2</sub>O/HTPB combustion products, obtained corresponding to its maximum adiabatic flame temperature values are shown in Table 3. It can be seen that the adiabatic flame temperature is maximum at an O/F ratio of 7.0.

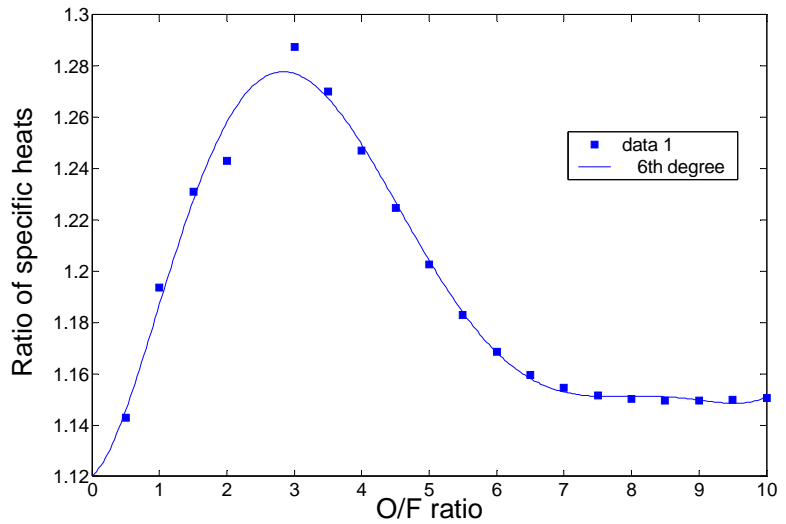


Figure 5. Ratio of specific heats vs. O/F ratio

Table 4 Motor geometry

Geometry	Values
Length of Grain(mm)	2000
Inner Diameter of Grain(mm)	135
Outer Diameter of Grain (mm)	164
Nozzle Throat Diameter (mm)	65
Area Ratio of the Nozzle	3
Oxidizer mass (kg)	51.7
Fuel mass (kg)	9.0135

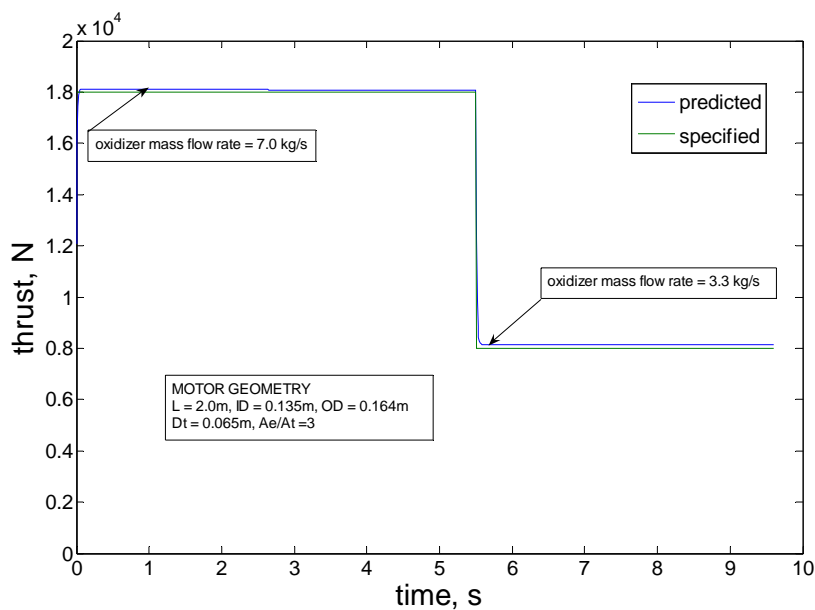


Figure 6. Predicted and specified thrust time profiles

In Fig. 6, predicted thrust time trace is compared with the specified one. The geometry of the motor arrived through the trial and error runs is given in Table 4. A good match is obtained for an oxidizer mass flow rate of 7.0 kg/s for the first phase. At 5.5 s the oxidizer mass flow rate is decreased to 3.3 kg/s to match the second phase of the specified thrust time profile.

Figure 7 shows the predicted pressure time trace. It is to be noted that the working pressure is below 45 bar so that the self-pressuring characteristics of  $N_2O$  may be explored for avoiding external pressurization. Figure 8 shows the predicted O/F ratios vs. time while in Fig. 9 the variation of specific impulse vs. O/F ratio is given. The mass flow rates of oxidizer, fuel and the total propellant are shown in Fig.10 and the required oxidizer mass calculated based on this is also given in Table 4. The predicted regression rate vs. oxidizer mass flux is shown in Fig.11 and this is the type of regression rate characteristics one must look for obtaining the specified thrust time profile for the motor geometry given in Table 4. Figure 12 shows the predicted nozzle exit plane pressure vs. time along with the ambient pressure. It can be seen that the exit pressure is always higher than the ambient pressure, thus avoiding any danger of flow separation due to over-expansion.

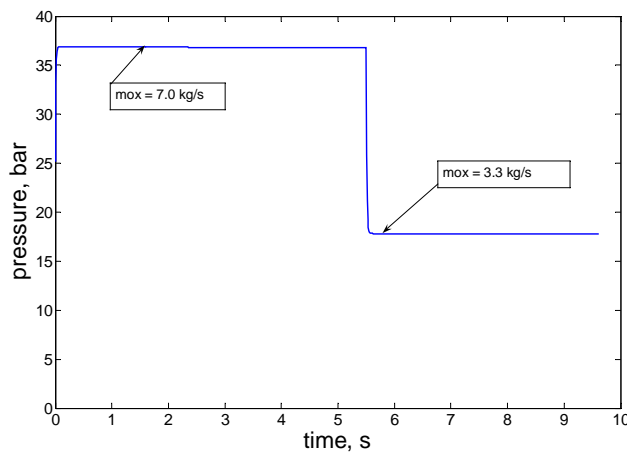


Figure 7. Predicted pressure time trace

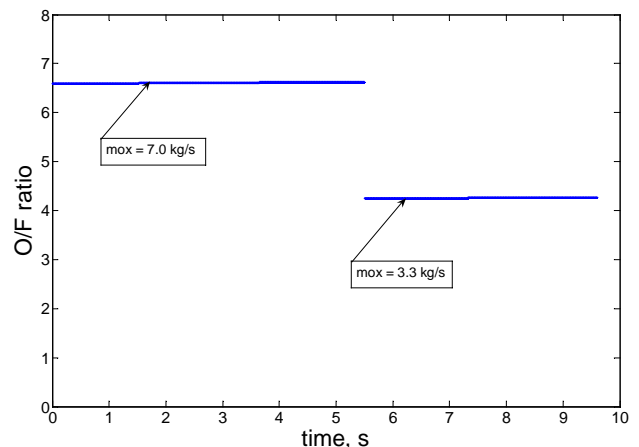


Figure 8. Predicted O/F ratio vs. time

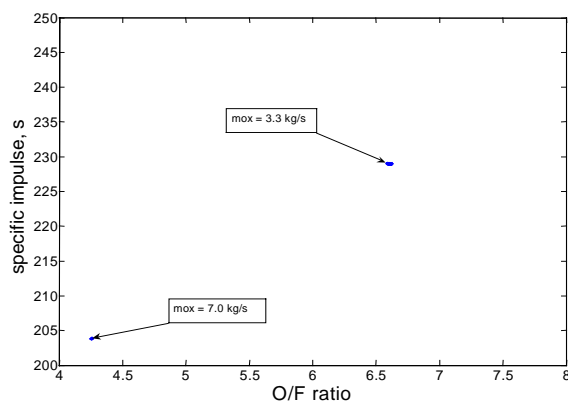


Figure 9. Predicted specific impulse vs. O/F ratio

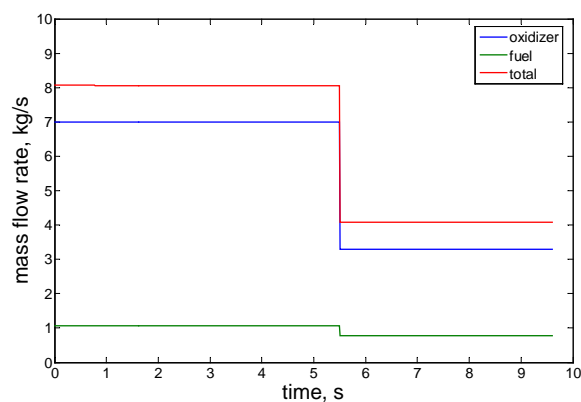
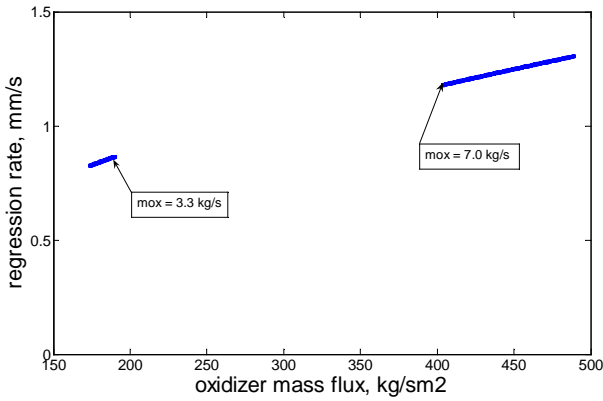
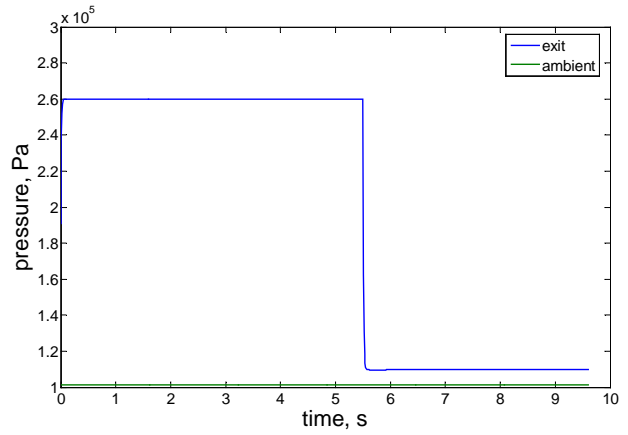


Figure 10. Predicted mass flow rates vs. time



**Figure 11. Predicted regression rate vs. oxidizer mass flux**



**Figure 12. Predicted exit pressure vs. time**

#### IV. Conclusions

The design details of a N<sub>2</sub>O/HTPB hybrid rocket motor for a specified thrust are described. The design of the motor is based on a code realized for predicting the performance of the hybrid rocket motor. Using the code, performance predictions can be obtained for a range of mass flow rates of the oxidizer assuming various motor geometries. The capability of the hybrid rocket motor for thrust modulation is demonstrated for a specified mission.

#### Appendix

Table 5 shows the specific impulse for an N<sub>2</sub>O and HTPB system calculated using the NASA CEA code at various O/F ratios ranging from 0.5 to 10.0. The area ratio assumed is 3 at a chamber pressure 70 bar. Assuming that the O/F ratio varies from 3.0 to 10.0 during the rocket motor operation, (operation below an O/F ratio of 3 will result in large losses of specific impulse), average values of specific impulse ( $I_{sp\_av}$ ) and O/F ratio ( $\phi_{av}$ ) can be computed. In the present case these values worked out to be  $I_{sp\_av} = 218.84$  s and  $\phi_{av} = 6.5$ . Using these values one can obtain the average values of the mass flow rates of oxidizer and fuel required for the thrust levels of both the phases, as follows

##### First Phase

$$\text{Total impulse} = \int F dt = \int_0^{5.5} (18000) dt = 18000 \times 5.5 = 99000 \text{ N.s}$$

Total average mass flow rate can be obtained as

$$\dot{m} = \frac{I}{I_{sp\_av} t_b}$$

where  $t_b$  is the burn duration

Now,

$$\dot{m} = \frac{99000}{218.84 \times 5.5 \times 9.8} = 8.39 \text{ kg/s}$$

**Table 5 Specific impulse of N<sub>2</sub>O/HTPB system**

Sr. No	O/F ratio	Isp, s
1	0.5	147.02
2	1.0	163.82
3	1.5	176.19
4	2.0	186.29
5	2.5	194.38
6	3.0	200.81
7	3.5	210.24
8	4.0	216.29
9	4.5	220.45
10	5.0	223.26
11	5.5	224.92
12	6.0	225.48
13	6.5	225.03
14	7.0	223.80
15	7.5	222.21
16	8.0	220.69
17	8.5	219.28
18	9.0	217.95
19	9.5	216.67
20	10.0	215.45

Now the oxidizer mass flow rate is obtained as

$$\dot{m}_{ox} = \frac{\dot{m}}{\left(1 + \frac{1}{\varphi_{av}}\right)} = \frac{8.39}{\left(1 + \frac{1}{6.5}\right)} = 7.27 \text{kg/s}$$

similarly the fuel flow rate

$$\dot{m}_f = \frac{\dot{m}}{(1 + \varphi)} = \frac{8.39}{(1 + 6.5)} = 1.12 \text{kg/s}$$

Second Phase

Total impulse =  $\int F dt = \int_0^{4.0} (8000) dt = 8000 \times 4.0 = 32000 \text{ N.s}$

Now total average mass flow rate can be obtained as

$$\dot{m} = \frac{8000}{218.84 \times 4.0 \times 9.8} = 3.73 \text{kg/s}$$

Now the oxidizer mass flow rate is obtained as before

$$\dot{m}_{\text{ox}} = \frac{\dot{m}}{\left(1 + \frac{1}{\phi_{\text{av}}}\right)} = \frac{3.73}{\left(1 + \frac{1}{6.5}\right)} = 3.23\text{kg/s}$$

similarly the fuel flow rate

$$\dot{m}_{\text{f}} = \frac{\dot{m}}{(1 + \phi)} = \frac{3.73}{(1 + 6.5)} = 0.4973\text{kg/s}$$

Oxidizer mass flow rates of 7.27 kg/s and 3.23 kg/s are taken as the first guesses in the trail and error computations for the first and second phases respectively.

### Acknowledgments

The author wishes to express his thanks to Dr. BSS Chandran, Head, Ramjet Propulsion Divison for the many useful discussions he had with him while doing this work.

### References

- <sup>1</sup>Krishnan, S., "Hybrid Rocket Technology: An Overview," *Third International High Energy Materials Conference and Exhibit*, Thiruvanthapuram, India, Dec.6-8, 2000, pp. 62-71.
- <sup>2</sup>Otto Krauss., " Design and Test of a Lab-Scale N<sub>2</sub>O/HTPB Hybrid Rocket " from the web site of University of Colorado at Boulder, USA.
- <sup>3</sup>George, P., et al., "Fuel Regression Rate in Hydroxyl-Terminated-Polybutadiene/Gaseous Oxygen Hybrid Rocket Motors," *Journal of Propulsion and Power*, Vol. 17, No. 1, January-February, 2001, pp. 35-42.
- <sup>4</sup>Wernimont, E. J., and Heister, S. D., "Combustion Experiments in Hydrogen Peroxide/Polyethylene Hybrid Rocket with Catalytic Ignition," *Journal of Propulsion and Power*, Vol. 16, No. 2, March-April ,2000, pp. 318-325.
- <sup>5</sup>Gordon, S., and McBride, B. J., "Computer Program for Calculation of Complex Chemical Equilibrium Compositions and Applications," *NASA Reference Publication 1311*.
- <sup>6</sup>Freedman, E., " Thermodynamic Properties of Military Gun Propellants," in *Stiefel, L., Gun Propulsion Technology*, Ch.5, US Army Armament Research, Development and Engineering Center Picatinny Arsenal, N.J.